Food Chemistry: X 27 (2025) 102495

Contents lists available at ScienceDirect

Food Chemistry: X

journal homepage: www.sciencedirect.com/journal/food-chemistry-x

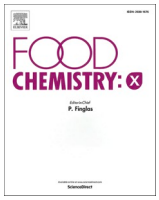

Curcumin-loaded gelatin/fucoidan electrospun composite: Physicochemical characterization and antioxidative application

Mohammad-Taghi Golmakani *, Elahe Zamansani, Mohammad Mahdi Hajjari, Marzieh Moosavi-Nasab, Mehrdad Niakousari

Department of Food Science and Technology, School of Agriculture, Shiraz University, Shiraz, Iran

ARTICLE INFO

Keywords:
Fucoidan
Gelatin
Hydrogen bonding
Molecular dynamics simulation
Oxidative potentiality

ABSTRACT

This study aimed to develop gelatin/fucoidan (GF) and curcumin-loaded gelatin/fucoidan (CGF) electrospun, enhancing the shelf life of food products as an active packaging material. Simulation studies indicated the conversion of collagen-like to gelatin-like peptides at ~75 °C and occurred hydrogen bonds between gelatin, fucoidan and curcumin. Morphological findings proved that optimum GF and CGF fibers had smooth and tubular morphology. Physicochemical results indicated possible hydrogen bonds between the compounds and enhanced thermostabilities using FTIR and TGA, respectively. Regarding antibacterial and antioxidant activities, CGF fibers demonstrated higher bactericidal (~8 and 11 mm) and antioxidative (~71 %) effects. During the 9-week storage test at 60 °C, lower values of PV and TBA values were observed for CGF and GF, endowing the peanuts decelerated lipid oxidation rate. These findings suggested a prospective active packaging material based on the incorporation of a bioactive molecule into a protein-carbohydrate composite, showing favorable active food packaging properties.

1. Introduction

Food packaging is a technique to reduce or overcome food spoilage caused by microbial growth or physical and chemical changes. These changes mainly affect food products' shelf-life, limiting their storage and transportation. Among these undesirable changes, lipid oxidation is one of the main reasons for reducing food products' quality and shelf-life by adversely altering their sensory properties and nutritional value (Pouralkhas, Kordjazi, Ojagh, & Farsani, 2023). Generally, food products such as peanuts with high content of unsaturated fatty acids demonstrate susceptibility to lipid oxidation, limiting the storage time and reducing their food quality (Golmakani et al., 2023). Peanuts is an important legume crop for their crucial role in human nutrition and food products. However, they exhibit susceptibility to lipid oxidation, containing a high amount of fats (45–50 %), comprising the majority of unsaturated fatty acids (80 % of total fatty acids). As reported, the main changes that occurred during the lipid oxidation of peanuts consist of the development of an off-flavor and a reduction of nutritional value (Kazemian-Bazkiaee et al., 2020; K. Liu, Liu, & Chen, 2019). Hence, food packaging materials with the ability to delay food products' oxidation have been immensely recommended. Despite the unique structure, abundance and cost-effectiveness of plastic-based packaging materials that decrease the chances of spoilage, biocompatible food packaging films and coatings are currently preferred owing to far fewer negative effects on the environment and health (Golmakani et al., 2023). In comparison with methods to fabricate biodegradable and packaging films, electrospinning is a straight-forward and an effective technique to generate fibers from biopolymers (Hajjari, Golmakani, & Sharif, 2023). Additionally, electrospinning has been highly recommended for encapsulation due to its dependence from temperature and pretreatments (Sharif, Golmakani, Hajjari, Aghaee, & Ghasemi, 2021). The examples of commonly electrospun proteins and carbohydrates are whey protein isolate and concentrate, zein, soy protein isolate, collagen, gelatin, pullulan, cellulose and chitosan. Gelatin is a protein derived from the denaturalization of collagen found in animal body parts (Pouralkhas et al., 2023). This protein is known as a cost-effective, nontoxic and biocompatible biopolymer with film-forming properties. Despite having promising features, some shortcomings such as thermosusceptibility, hydrophilicity, structural weakness, and poor moisture barrier properties limit the applications of gelatin. Nonetheless, it is suggested that gelatin should be supported by copolymers or other constituent to overcome the drawbacks (Amani, Rezaei, Akbari, Dima, &

* Corresponding author at: Department of Food Science and Technology, School of Agriculture, Shiraz University, Shiraz 7144165186, Iran.
E-mail addresses: golmakani@shirazu.ac.ir (M.-T. Golmakani), marzieh.moosavi-nasab@mail.mcgill.ca (M. Moosavi-Nasab).

https://doi.org/10.1016/j.fochx.2025.102495
Received 21 December 2024; Received in revised form 17 April 2025; Accepted 22 April 2025
Available online 23 April 2025

Jafari, 2022). For instance, Zhou et al. (2020) evaluated essential oil-loaded gelatin fibers with improved water barrier function for packaging application. Moreover, Luo et al. (2022) reported studies on the active food packaging application of gelatin-based films for coating fruits, vegetables, fish and meats.

Fucoidan is a polysaccharide containing high amounts of L-fucose and sulfate ester groups extracted from brown seaweed. There have been numerous studies on applications of fucoidan for its medically and non-medically potential properties, while, this compound has not modified and suggested as pure material for electrospinning process (Ho, Lim, Kim, Kim, & Chun, 2023; Zhao, Garcia-Vaquero, Przyborska, Sivagnanam, & Tiwari, 2021). Ashayerizadeh, Dastar, and Pourashouri (2020) reported that fucoidan has also antibacterial and antioxidant activities, however, their effects depend on chemical groups and applied dosage. Pouralkhas et al. (2023) stated that fucoidan can demonstrate bactericidal effects against *E. coli* and *S. aureus*. Therefore, this compound has recently gained growing attentions to be used in food applications. For instances, Wang et al. (2023) studied anthocyanin-loaded chitosan/fucoidan film for food packaging application. They stated the utilization of fucoidan improved the physical and biological properties because of occurred cross-links. Perera, Sharma, Pradhan, Jaiswal, and Jaiswal (2021) reported that chitosan-alginate films containing fucoidan had better barrier properties and higher antioxidant effects. Curcumin with a chemical formula of $C_{21}H_{20}O_6$, as an environmentally-safe phenolic compound, is known for its biodegradable, biocompatible, antimicrobial and antioxidant properties. Due to its unique characteristics, hydrophobic curcumin has been widely used as flavor and coloring pigment in the food applications (Akman, Bozkurt, Balubaid, & Yilmaz, 2019). Moreover, polyphenol compounds exhibit facile incorporation mainly owing to their noncovalently affinity towards polysaccharides and protein using their terminal hydroxyl groups (Hajjari & Sharif, 2022). However, its low bioavailability, instability, water insolubility, and rapid degradability restricts its facile applications (Zheng, Yao, & Chen, 2022).

The aim of this study was to develop and investigate active food packaging fibers based on electrospun curcumin-loaded gelatin-fucoidan. Additionally, to ascertain the optimum condition, various ratios of compounds in a same condition were tested. Three-dimensional structures were obtained and modeled based on modeling, molecular dynamics and docking simulations. Then, the fibers were characterized by morphological, physicochemical and packaging application tests. In addition to the mentioned experiments, antibacterial effects against *Escherichia coli* and *Staphylococcus aureus* as well as antioxidant activity against free radicals were evaluated. Hence, a promising active food packaging material based on protein-carbohydrate interactions was comprehensively surveyed.

2. Materials and methods

2.1. Materials

Fucoidan was purchased from Bio-tech (Beijing, China). Gelatin (type B), Curcumin, glacial acetic acid, trichloroacetic acid, thiobarbituric acid, aluminum chloride, sodium carbonate, potassium acetate, butylated hydroxytoluene (BHT), gallic acid, quercetin, Folin-Ciocalteu reagent, sodium 1,2-naphthoquinone-4-sulfonate, 2,2-diphenyl-1-picrylhydrazyl (DPPH), and tryptic soy agar (TSA) were bought from Sigma-Aldrich (St. Louis, MO). All chemicals were of analytical grade.

2.2. Solution preparation

The preparation of solutions containing gelatin, fucoidan, curcumin and aqueous acetic acid (70 %, *w/v*) had three consecutive stages. Firstly, pristine gelation and fucoidan solutions (22 %, *w*/w) were made by dissolving in aqueous acetic acid. Then, gelatin:fucoidan solutions (22 %, w/w) with various ratios of 1:1, 1:2, 1:3, 2:1 and 3:1 were prepared. Lastly, optimum gelatin:fucoidan samples were mixed with curcumin at various concentrations of 20 %, 30 % and 40 % w/w.

2.3. Fabrication of fibers

The fibers were generated by an electrospinning machine (Spinner-3×-Advance, ANSTCO, Iran). The process was carried out with a voltage of 16 kV, flow rate of 1 mL/h, collector distance of 10 cm in ambient conditions (at 25 °C).

2.4. Simulation studies

Before performing the experiments on fibers, molecular modeling, dynamics (MD) and docking simulations were performed to elucidate the compounds' behavior during the experiments. Regarding molecular modeling, fucoidan (five $\alpha_{1\rightarrow3}$-L-fucopyranose compounds entailing the sulfate ester group at C2) and curcumin were obtained from carbohydrate builder of GLYCAM-web (Woods, 2005) and Automated Topology Builder (Malde et al., 2011), respectively. Due to the lack of gelatin 3D model, there is a necessity to model or predict the structures based on homology or ab-initio modeling methods (Hajjari & Sharif, 2024). In addition, triple helical collagen-like peptide (ID: 1BKV) was obtained from RSCB PDB (Kramer, Bella, Mayville, Brodsky, & Berman, 1999). Collagen peptide was used to mimic collagen to gelatin thermal conversion. Two MD simulations were performed in this study. First, collagen was added to the centre of a simulation box filled with water where there were distances of 1 nm between the protein and edges under a periodic boundary condition. Then, steps of Ionic neutralization and energy minimization (steepest descent method), N*V*T (~350 K, 0.5 ns, Nosé–Hoover thermostat), NPT (0.5 ns, Parrinello-Rahman barostat) ensembles and MD run (20 ns, GROMOS 54A7 force field). GROMACS (University of Groningen, Version 2019.6, Groningen, Netherlands). After the first MD simulation, randomly structured gelatin-like peptides were exploited for a molecular docking simulation. Therefore, fucoidan-gelatin and curcumin-fucoidan-gelatin structures were set for 50 random conformations using AutoDock (Scripps Research, Version 4.2, San Diego, CA) and Lamarckian genetic algorithm to find their potential affinities. Second, same parameters were chosen for the latter MD simulation on a gelatin-like peptide with some changes in solvent (acetic acid), NVT (~300 K, V-rescale thermostat) and electric field (1 V/nm) for a 10 ns simulation run. This simulation was to understand the behavior of gelatin-like peptide under an electric field. Eventually, structures were visualized by VMD (University of Illinois Urbana-Champaign, Version 1.9.3, Champaign, IL) and Molegro Virtual Docker (CLC bio, Version 6.0, Aarhus, Denmark). MD results of intermolecular hydrogen bonds, RMSD and radius of gyration in z direction (R_g) were also reported.

2.5. Characterization of fibers

2.5.1. Morphological properties

Morphological study of fibers was performed using the analyses of images taken from scanning electron microscope (SEM) (TESCAN, Brno, Czech Republic). The Digimizer (Version 5.3.5, Ostend, Belgium) measurements were selected at 100 random points ($n = 100$) for each sample. Encapsulation efficiency (EE%) of curcumin in curcumin-loaded fiber was measured using a method described by Akman et al. (2019) as firstly 20 mg of fiber was dissolved in 10 mL of PBS. Secondly, the solution was centrifuged for 10 min at 4000 rpm. Ultimately, the absorbance of liquid phase was read at wavelength of 428 nm. The percentage of EE was therefore calculated using the following equation.

$$\text{Encapsulation efficiency } (\%) = ((\text{E–n} - \text{E})/(\text{E})) \times 100 \quad (1)$$

where E and n-E were corresponding to the hypothetically encapsulated

and actually non-encapsulated amounts (mg) of the curcumin in the composite, respectively.

2.5.2. Physicochemical properties

The functional groups and chemical structure of samples were studied by a Fourier-transform infrared spectroscope (FTIR) (Tensor II, Bruker, Germany), recording data from 4000 to 400 cm^{-1}. In addition, changes in crystallinity of samples were studied via X-ray diffraction technique (XRD) (D8 ADVANCE, Bruker, Bremen, Germany), when the Cu Kα radiation was used and data were recorded in the 2θ range of 5–80°. The thermostability of samples was evaluated using a thermogravimetric analyzer (TGA) (DSC/TGA1, Mettler Toledo, Switzerland) in an inert condition during a gradual heating up from 30 to 600 °C with a rate of 10 °C/min.

2.6. Functionality of fibers

2.6.1. Antioxidant activity

DPPH assay was applied to understand free radical scavenging activity of samples. In brief, 30 mg of GF and CGF were mixed with 5 mL of 0.1 M methanolic DPPH solution (control samples were also used without the presence of GF and CGF). After keeping the samples in ambient conditions and dark, the absorbance values were read at 517 nm and the following equation was used to calculate the percentage of the antioxidative activity.

$$\text{Antioxidative effect}\ (\%) = ((A_C – A_S)/(A_C)) \times 100 \quad (2)$$

where A_C and A_S were the absorbance values of the control and samples, respectively.

2.6.2. Antimicrobial activity

Disk diffusion method as the indication of inhibitory effects of samples on the growth of bacteria was performed (Golmakani et al., 2023). In this regard, PBS solutions containing *E. coli* and *S. aureus* bacteria with a concentration of 10^6 CFU/mL were prepared. The absorbance value of solutions was set to the values in a range of 0.08 to 0.1 at 600 nm to comply with McFarland's turbidity standard. On the plates containing TSA culture medium, 100 μL of bacterial solutions were spread. Moreover, UV-sterilized samples with a diameter of 2 cm were placed in the centre of plates. All plates were kept in an incubation for 24 h at 37 °C. Finally, fibers' bactericidal inhibition zones were measured.

2.7. Application of fibers

2.7.1. Oxidative potentiality and accelerated storage test

Oxidative potentiality of samples was investigated based on the oil efficiency of peanuts samples. Therefore, 10 g of peanuts were manually coated with filtration papers to mix with hexane in a Soxhlet apparatus. The remaining hexane was evaporated by an oven at a temperature of 40 °C for 24 h. The oil efficiency was calculated based on the weight differences. Moreover, an accelerated storage study during a 9-week test was performed. In this regard, 20 g of peanuts were manually coated (peanuts were wrapped by fibers) with 30 mg of fibers to be kept at a temperature of 60 °C (Golmakani et al., 2023).

2.7.2. Peroxide value test

Primary oxidation products were measured using peroxide value (PV) test. Therefore, ~0.01–0.03 g of hexane-extracted peanuts oil was mixed with ~10 mL of chloroform:methanol mixture (~2.5:1). Then, ~50 μL of ammonium thiocyanate and iron chloride was added to then solution. Finally, sediments were formed after the addition of ~100 μL of 1 M HCl. The absorbance was read at 500 nm and PVs were calculated using the following equation (Sabaghi, Maghsoudlou, Khomeiri, & Ziaiifar, 2015).

$$\text{Peroxide value} = ((A_S – A_C) \times S)/(amu_{Fe} \times 2 \times m_S) \quad (3)$$

where A_S, A_C, S, amu_{Fe}, and m_S are absorbances of the sample and control, slope obtained from the calibration curve (41.52), atomic mass of iron (55.84), and the mass of the sample (g), respectively.

2.7.3. Thiobarbituric acid test

Secondary oxidation products were measured using thiobarbituric acid (TBA) test. Based on this method, ~0.01–0.03 g of hexane-extracted peanuts oil and trichloroacetic acid (~15 g) were dissolved in a mixture containing thiobarbituric acid (~0.3 g), HCl (1.76 mL, 12 M) and distilled water (82.8 g). Then, 3 mL of 2 % butylated hydroxytoluene: ethanol with an equal ratio was added to the solution. This mixture was remained in boiling water bath for 15 min and sediments were separated from liquid phase by centrifugation at the speed of 3500 rpm for 10 min. Finally, the absorbance value of liquid phase was measured at 532 nm (Siripatrawan & Harte, 2010).

2.8. Statistical analysis

All results were reported with mean values ± standard deviation of at least triplicate determinations ($n \geq 3$). SPSS 26 statistical software (SPSS Inc., Chicago, IL) was used to evaluate statistical analyses via one-way ANOVA with Tukey's post-hoc test. Duncan's multiple range test with a 95 % level of probability ($P < 0.05$) was used to measure the significant differences.

3. Results and discussion

3.1. Simulation

Simulation studies were carried out to display a deeper understanding of the changes and interaction between compounds. Molecular dynamics and docking simulation results are reported in Fig. 1. According to the Fig. 1a, fucoidan was successfully docked with the three-dimensional structure of gelatin-like peptide obtained from the thermal denaturation of collagen-like peptide. Two occurred phenomena were as follows: (i) The thermal denaturation of collagen destroyed hydrogen bonds between collagen chains and therefore loss of its initial triple-helix form (Abdullah et al., 2018; Ahmad et al., 2020). Similar result was reported by Ravikumar, Humphrey, and Hwang (2007) where temperature of ~57 °C was applied on the collagen-like peptide. In this regard, Molegro showed that collagen peptide had 24 hydrogen bonds which diminished to 8 of two remaining chains. In addition to hydrogen bonds, steric interactions are shown in Fig. S1. RMSD and R_g results in Fig. S2a-b were also in accordance with Fig. 1 findings where RSMD showed incremental instability owing to the applied stress. Additionally, R_g values gradually decreased, proving its more negligible folding than native form of its chain (Hajjari & Sharif, 2021). (ii) Two conformations with highest binding affinities showed that fucoidan molecules were docked by hydrogen bonds with gelatin-like peptide's proline residue numbers of 10, 14, 16 and 20. Moreover, glycine 9, 12 and proline 1 were the target sites of curcumin to with gelatin-like peptide via hydrogen bonds (Fig. S3). Although curcumin molecules showed affinities towards fucoidans (Fig. S4), top three docking conformations indicated the interactions between curcumin and gelatin. In the second MD simulation, the applied electric field (1 kV/nm) on the protein resulted in an elongated structure as significantly changed RMSD and R_g values (Fig. S2c-d). This was an indication of the gelatin-like peptide under an electric field.

3.2. Morphological and physicochemical properties

Fig. 2 shows the SEM images of samples. According to Fig. 2, all fibers had tubular (ribbon-like) shape. Hajjari et al. (2023) reported that

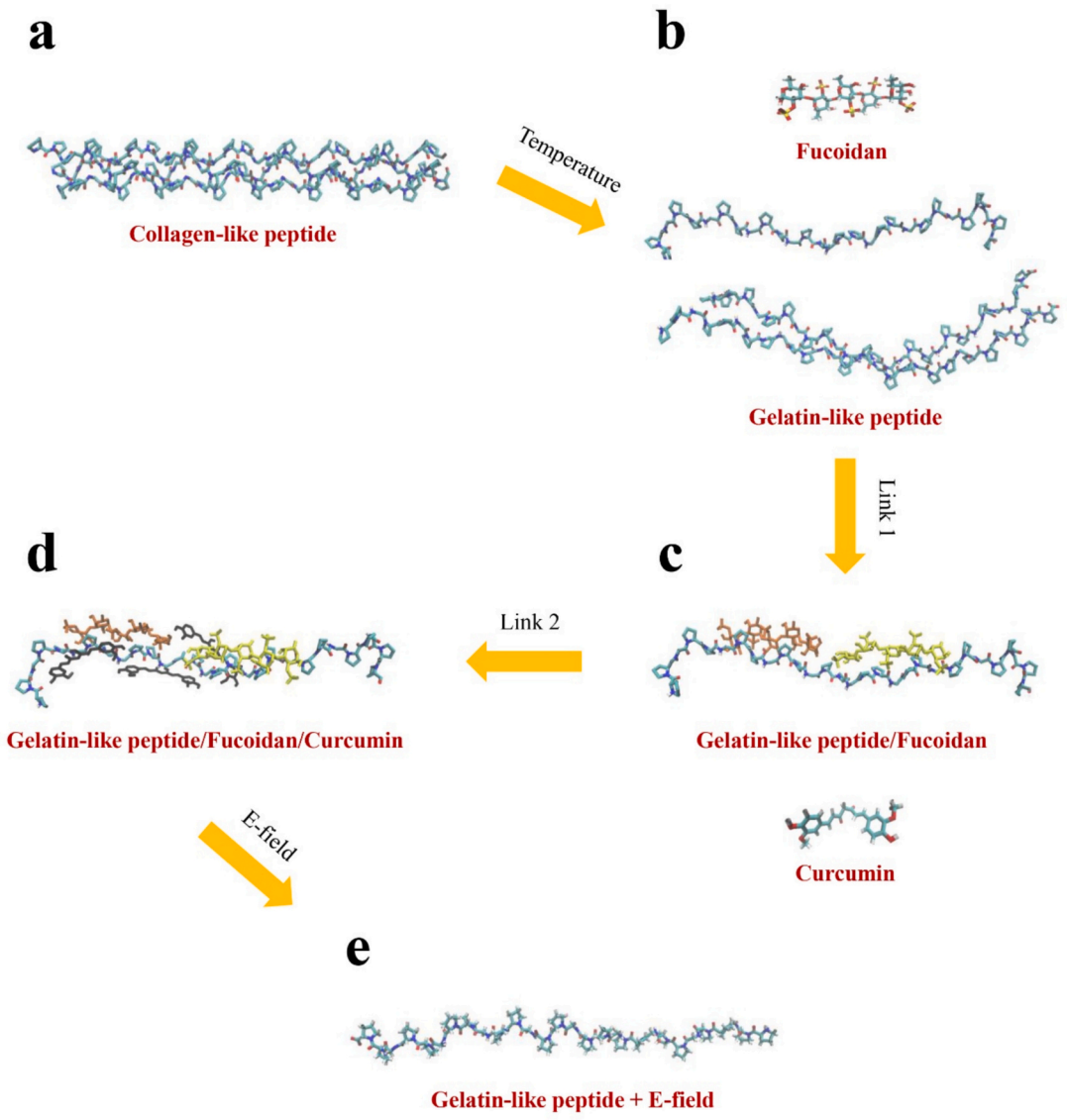

Fig. 1. (a) Molecular dynamics of collagen-like peptide at ~75 °C. (b) Molecular docking of (b) gelatin-like peptide with fucoidan and (c) gelatin-like peptide/fucoidan with curcumin. (d) Three-dimensional structure of gelatin-like peptide/fucoidan/curcumin. (e) Gelatin-like peptide under an electric field of 1 kV/nm.

tubular shape of fiber would be obtained from the denaturation of protein caused by the occurrence of the hydrogen bonds between protein and acid molecules. In spite of the smooth, unbeaded and unbranched morphology of most of samples, a few samples where there was a dominance of fucoidan over gelatin were not properly processed, indicating high number of beads and branches across the fibers. Measurements of fibers' diameter displayed that gelatin:fucoidan complexes had approximately same average dimeters around 400 nm, respectively. In addition, incorporation of curcumin into the metrices showed increases in diameter as measured 314 ± 61, 383 ± 21 and 450 ± 22 nm for curcumin-loaded gelatin:fucoidan (20 % loading, 3:1), curcumin-loaded gelatin:fucoidan (30 % loading, 3:1) and curcumin-loaded gelatin:fucoidan (40 % loading, 3:1), respectively. Accordingly, gelatin:fucoidan (3:1) and curcumin-loaded gelatin:fucoidan (40 % loading, 3:1) fibers were selected as the optimum samples based on the smooth morphology and highest amount of loaded-curcumin. The optimum electrospun fibers were also named as follows: GE, GF and CGF for the fibers of pure gelatin, gelatin:fucoidan (3:1) and curcumin-loaded gelatin:fucoidan (40 % loading, 3:1), respectively. It is worth noting that, CGF had a curcumin encapsulation efficiency of 90.6 ± 2.5 %.

Fig. 3a shows FTIR spectra and TGA thermograms of samples. FTIR spectrum of curcumin indicated significant peaks at ~3300 cm^{-1} (hydroxyl groups), ~1640 cm^{-1} (carbonyl groups) and ~ 1530 cm^{-1} (ethylene groups). In addition, other negligible peaks between 1400 and 1500 cm^{-1}, at 1250, between 800 and 1000 cm^{-1} were attributed to −C − O elongation of the O − H, ether and alkene groups, respectively (Roy & Rhim, 2020). For fucoidan structure, several distinctive peaks at ~3350 cm^{-1} (hydroxyl groups), ~1612 cm^{-1} (C—O of carboxylic acid groups), ~1250 cm^{-1} (O=S=O of sulfate esters), at ~1020 cm^{-1} (S=O of sulphoxides) and between ~820–910 cm^{-1} (C–O–S of sulfate groups) were observed (Ho et al., 2023; Zhao et al., 2021). Moreover, proteins generally have three characteristic peaks of amides A, I, II and III (Hajjari et al., 2023). Accordingly, amide A peak (N—H and hydrogen bonding), amide I (C=O and hydrogen bonding corresponding to COO−), amide II (C—H and $-NH3^{+}$) and amide III (C—N, N—H or CH_2 groups of glycine) of gelatin were found at ~3300, 1650, 1540 and 1460 cm^{-1} (Pouralkhas et al., 2023). According to the findings, after electrospinning amide I peaks of GF and CGF were shifted from ~1650 cm^{-1} to higher wavenumbers ~1660 cm^{-1} which might be due to proteins' unfolding and changes in secondary structure. These shifts also could be the results of hydrogen bonds occurred between fucoidan-

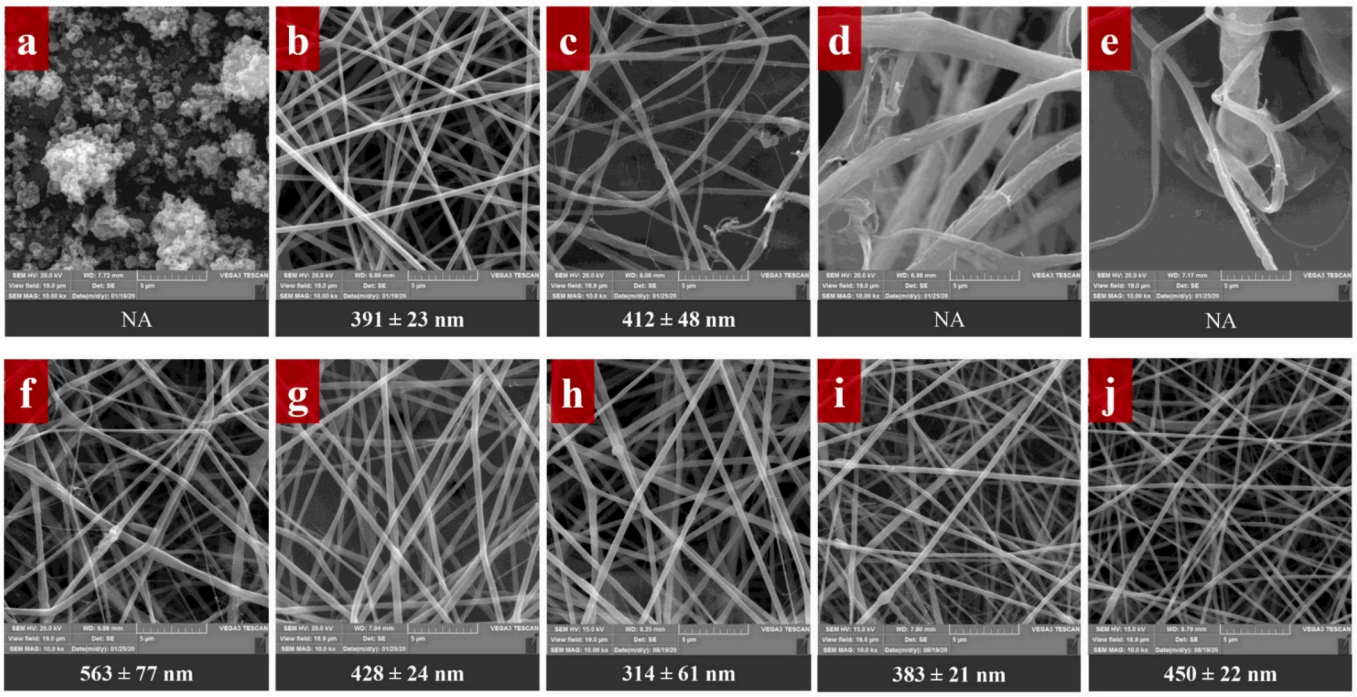

Fig. 2. SEM images of (a) fucoidan fiber (22 %, *w*/w), (b) gelatin fiber, (c) gelatin:fucoidan (1:1), (d) gelatin:fucoidan (1:2), (e) gelatin:fucoidan (1:3), (f) gelatin:fucoidan (2:1), (g) gelatin:fucoidan (3:1), (h) curcumin-loaded gelatin:fucoidan (20 % loading, 3:1), (i) curcumin-loaded gelatin:fucoidan (30 % loading, 3:1), (j) curcumin-loaded gelatin:fucoidan (40 % loading, 3:1).

gelatin and curcumin-fucoidan-gelatin compounds as also reported in simulation part of this study (section 3.1) (Hajjari, Golmakani, & Sharif, 2021). Hajjari and Sharif (2021) studied proteins' structural changes during denaturation and unfolding when they were dissolved in a proper solvent and affected by high electric fields. Accordingly, as also stated in section 3.1, electric field elongated the protein and was able to alter the protein conformation.

XRD of samples are shown in Fig. 3b. According to this figure, the amorphous structure of protein-based samples was found via their broad humps (Hajjari, Golmakani, & Sharif, 2021). Additionally, fucoidan sample exhibited a diffraction pattern, proving its amorphousness. The similar finding regarding the XRD pattern of fucoidan was previously reported by Mani et al. (2024). In contrast, curcumin had sharp Bragg reflections. Generally, these sharp peaks are indications of crystalline nature of the sample (Akman et al., 2019). Therefore, it was expected that the only electrospun fiber with crystalline nature could be CGF. Interestingly, after the incorporation of curcumin in gelatin/fucoidan (i.e., CGF), the main peaks of curcumin were diminished except the one at about ~18°. Hence, the XRD pattern of CGF might explain two scenarios. First, the peak at ~18° proved the presence of curcumin in the resultant fiber. Second, the curcumin molecules were successfully incorporated by intermolecular interactions with amorphous gelatin/fucoidan as most of sharp peaks were disappeared.

Thermograms of samples are observed in Fig. 3c. As shown, curcumin was thermally stable, however, its thermostability gradually decreased after ~250 °C. Similar results regarding the thermostability of curcumin was reported by Masek, Chrzescijanska, and Zaborski (2013). They also mentioned that this thermal stability proved the resistance of curcumin molecules against adverse changes during technological processes. The destruction of the polysaccharide macromolecule by increasing temperature is followed by three and four levels. Regarding fucoidan, it had the first level of physically absorbed water evaporation at ~70 °C. In the second phase in a range of 220–280 °C, fucoidan started to lose chemisorbed water and fucoidan molecular structure simultaneously. Fucoidan's curve ultimately underwent a random breakage of glycosidic linkages after 400 °C (Pouralkhas et al., 2023). Generally, proteins' thermograms include two determinative weight losses: (i) when the unbound water molecules and volatile compounds are evaporated and (ii) when decomposition occurs in proteins' structure (Sharif, Golmakani, & Hajjari, 2022). Finding proved that gelatin possessed remarkable decreases at ~80 and 260 °C. Similar results were reported by Roy and Rhim (2020) where weight losses at ~90 and ~300 °C were attributed to the evaporation of moisture and degradation of gelatin matrix, respectively. Based on the results, it was proven that fucoidan and curcumin were able to increase the thermostability of gelatin and gelatin-fucoidan, respectively. As demonstrated, CGF had the more thermostability than gelatin, fucoidan and GF. In addition to this, Hajjari, Golmakani, Sharif, and Niakousari (2021) attributed a negligibly thermostabilized fibers to the reduced hygroscopicity after electrospinning process. Hence, Pouralkhas et al. (2023) reported that fucoidan was capable of improving the thermostability of gelatin by possible electrostatic interactions between biopolymers.

3.3. Antimicrobial and antioxidant activities

Table 1 indicates the antibacterial and antioxidant activities of GF and CGF. As shown in Table 1, antibacterial activities of GF and CGF against *S. aureus* were more effective than against *E. coli*. CGF inhibited *S. aureus* and *E. coli* with the inhibitory zones of 11.3 ± 1.3 and 8.3 ± 0.5 mm, respectively. GF's bactericidal activity against *S. aureus* and *E. coli* were 7.9 ± 1.5 and 5.7 ± 0.7 mm, respectively. Antibacterial activity of CGF against *S. aureus* and *E. coli* are shown in Fig. S5. These findings revealed that the fibers had an incremental activity when curcumin incorporated. Golmakani et al. (2023) reported that *E. coli* bacteria were able to hinders the diffusion and penetration of macromolecules and hydrophobic compounds across its membrane due to hydrophilic surface of LPS layer. This feature might be the reason of the diminished susceptibility of *E. coli* during bacterial tests. Although gelatin possesses no enough antibacterial properties (Zhou et al., 2020), GF's and CGF's antibacterial activities were mainly attributable to fucoidan and the combination of fucoidan-curcumin, respectively. Bactericidal mode of action of fucoidan is still unclear. However,

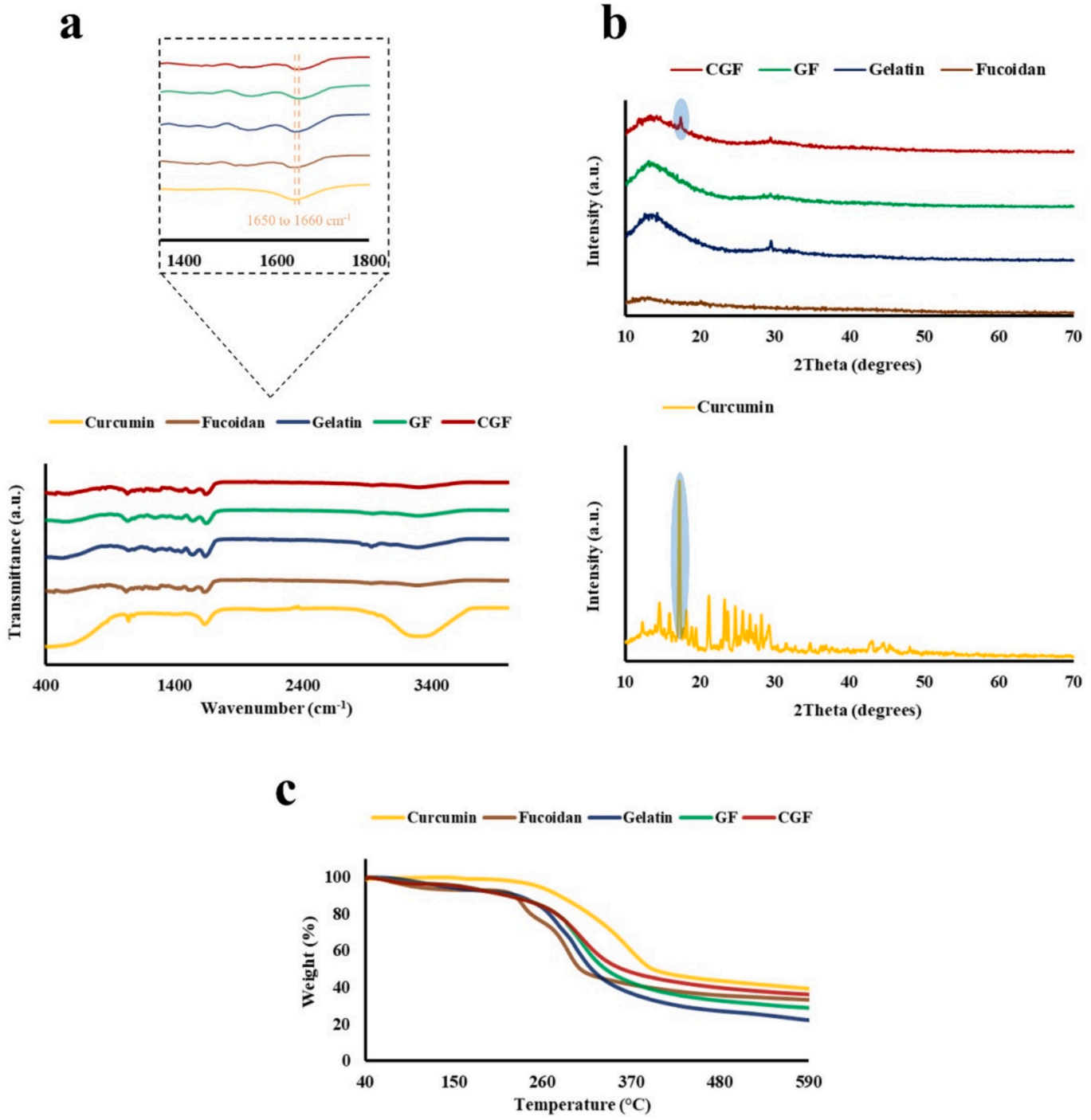

Fig. 3. (a) FTIR and (b) XRD spectra as well as (c) TGA thermograms of curcumin, fucoidan, gelatin, GF (gelatin:fucoidan, 3:1), and CGF (curcumin-loaded gelatin: fucoidan, 40 % loading, 3:1).

Table 1
Antioxidative and bactericidal activities of GF and CGF.

Sample	Aantioxidant activity (%)	Antibacterial activity (mm)	
		Staphylococcus aureus	*Escherichia coli*
GF	50.4 ± 9.7^{a}	7.9 ± 1.5^{a}	5.7 ± 0.7^{a}
CGF	71.5 ± 5.5^{b}	11.3 ± 1.3^{b}	8.3 ± 0.5^{b}

Means with different letters are significantly different ($P < 0.05$). GF and CGF are gelatin-fucoidan and curcumin-loaded gelatin/fucoidan composites, respectively.

inhibitory pathways of fucoidan against *S. aureus* and *E. coli* can be connected with two scenarios of (i) disruption of the cell membrane, leakage of interior components and elimination of cells and (ii) entrapment and reduction of nutrients in the culture medium including cationic minerals by fucoidan's negatively charged feature (M. Liu et al., 2017). Regarding curcumin bactericidal activity, curcumin molecules can suppress cell division, cause cell membrane's permeability and subsequently eliminate bacterial cells (Luo et al., 2022). Similarly, Roy and Rhim (2020) reported curcumin molecules can interrupt the FtsZ's function which matters during cell division.

In Table 1, CGF (71.5 ± 5.5 %) demonstrated a higher antioxidant

activity than GF (50.4 ± 9.7 %). According to Akman et al. (2019); Ashayerizadeh et al. (2020), both fucoidan and curcumin are involved in high free radical scavenging effects by their proton-donating ability. Hence, CGF might have two simultaneous antioxidant activities when exposure to DPPH solution. It is worth noting that synergistic antioxidant effect of fucoidan and curcumin could be observed. Accordingly, Hifney, Fawzy, Abdel-Gawad, and Gomaa (2016) stated that the fucoidan's antioxidant capacity is strongly related to polyphenol content. They proved that antioxidant activity of had connection with the contents of fucose (for their methyl active groups), uronic acids and polyphenol for fucoidan's radical scavenging property. Akman et al. (2019) also reported that curcumin proved its effect because of the abundance of hydroxyl groups on its phenolic structure and hydrogen detachment from the methylene CH_2 group that present in curcumin molecules. Roy and Rhim (2020) stated similar increased antioxidant activity because of curcumin molecules' phenol group.

3.4. Oxidative stability

Fig. 4 indicates PV and TBA values of coated and uncoated peanuts. Peroxides and hydroperoxides are the indices of lipid oxidation's initial products. As shown, PVs of coated and uncoated peanuts increased throughout the 6-week storage period. These increments meant that the all samples begun their lipid oxidation. Despite the incremental trend, PVs after 6th week had a downward trend. This phenomenon was assumed to be connected with the first steps of lipid oxidation affect chain reactions, forming hydroperoxides as primary lipid oxidation products which could decompose to secondary lipid oxidation products (Sangatash, Niazmand, Jamab, & Modaressi, 2016). Generally, PVs below 10 meq/kg, as acceptable peroxide value, confirms food products' freshness during the storage period (Liu et al., 2019). Accordingly, all samples before the break point in 6th week demonstrated PVs below 10 meq/kg. Interestingly, control, GE and GF samples had the steeper curves from the beginning, affirming their accelerated rate to produce the initial oxidation products (Kazemian-Bazkiaee et al., 2020). Therefore, CGF had the best coating functionality than other samples, whereas GF was placed second. Similar PVs' trend on peanuts samples was also observed by Kazemian-Bazkiaee et al. (2020); K. Liu et al. (2019); Sangatash et al. (2016).

Secondary lipid oxidation products such as aldehydes and carbonyl, mainly developing off-odor of oils, are formed by the degradation of peroxides and hydroperoxides (Sangatash et al., 2016). As mentioned, this degradation might be the reason of the downward trend observed in PV curves after 6th week. Similar to the PV findings, TBA curves increased during the storage period. The increases gradually continued until 6th week. Hence, as expected, the coated samples in particular CGF and GF revealed less increasing rate of TBA values compared to other samples. After 6th week, sharp increments were observed in TBA values which could be the effects of degradation of lipid oxidation's primary products. Golmakani, Hajjari, Kiani, Sharif, and Hosseini (2024); Golmakani et al. (2023) reported similar PV and TBA curves' trends when they investigated lipid oxidation of coated and uncoated walnut kernels. Based on the PV and TBA results, it could be concluded that both GF and CGF were able to reduce lipid oxidation due to their antioxidant effects. Based on the comparison between GF and CGF, GF slightly decreased the rate of oxidation probably owing to its negligible barrier properties. It is worth noting that despite the substantial role of antioxidative agents, strong UV-absorption feature of the phenol groups in curcumin structure and increases in coating's thickness and number of layers due to the alteration of barrier properties can also affect oxidation rate of samples (Sangatash et al., 2016; Zhang et al., 2021). Moreover, K. Liu et al. (2019) measured that the temperature- and time-dependent peanuts storage tests caused lipid oxidation along with the alteration of the fatty acid composition. Interestingly, Luo et al. (2022) reported various applications of gelatin-based coating material on fruits, vegetables, fish and meats.

4. Conclusion

Gelatin-fucoidan electrospun composites with (CGF) and without (GF) curcumin were successfully fabricated. Simulation results firstly provided the structure of gelatin-like peptide docked with fucoidan and curcumin by hydrogen bonds. Secondly, MD simulation proved the gelatin-like peptide elongation under an electric field, mimicking the applied field provided during electrospinning process. SEM images revealed tubular morphology of GF and CGF fibers. Moreover, CGF had the encapsulation efficiency of 90.6 ± 2.5 %. Physicochemical studies stated that chemical and structural changes occurred during electrospinning. XRD patterns of the samples demonstrated the presence of crystalline curcumin in amorphous structures of gelatin and fucoidan. In addition to this, fucoidan and curcumin were able to enhance the thermostabilities of gelatin and gelatin-fucoidan fibers, respectively. As expected, CGF had higher antioxidant and antibacterial effects probably due to the incorporation of curcumin. However, GF also proved its activities owing to the presence of fucoidan. Ultimately, 9-week storage application of fibers using PV and TBA tests confirmed that coated peanuts had lower PV and TBA values, stating a decreasing rate of lipid oxidation. In this technique, CGF's PV and TBA curves was less steep compared to those of other samples. It was believed that the combination of the reported findings could suggest a promising electrospun composite to be effectively applied on food product as an antioxidative food packaging material.

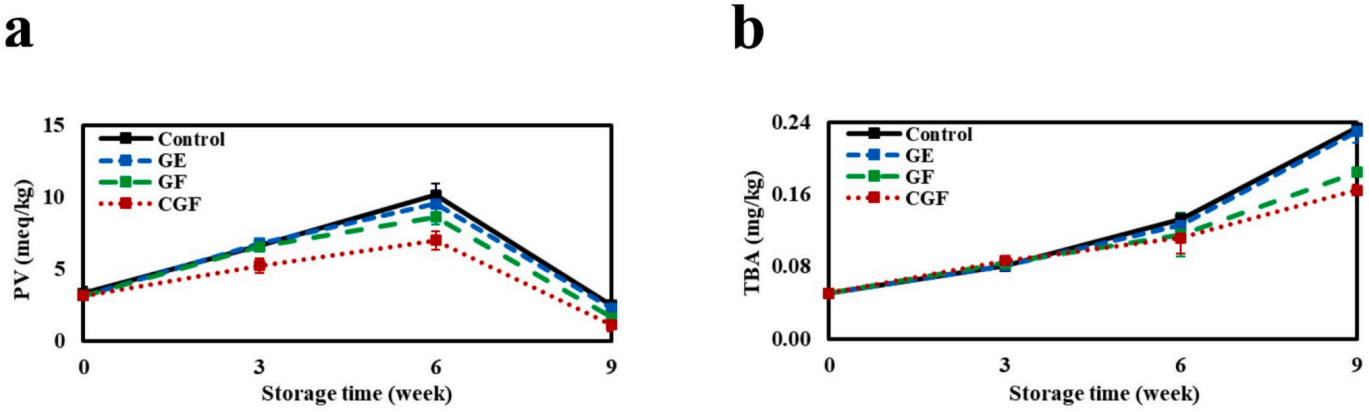

Fig. 4. (a) Peroxide value (PV) and (b) thiobarbituric acid (TBA) of uncoated peanut samples and coated samples with gelatin fiber (GE), GF (gelatin:fucoidan, 3:1), CGF (curcumin-loaded gelatin:fucoidan, 40 % loading, 3:1) during the accelerated storage period.

CRediT authorship contribution statement

Mohammad-Taghi Golmakani: Writing – review & editing, Visualization, Validation, Supervision, Resources, Project administration, Funding acquisition, Conceptualization. **Elahe Zamansani:** Writing – original draft, Software, Methodology, Investigation, Formal analysis, Data curation. **Mohammad Mahdi Hajjari:** Writing – original draft, Visualization, Validation, Software, Methodology, Investigation, Formal analysis, Data curation, Conceptualization. **Marzieh Moosavi-Nasab:** Supervision. **Mehrdad Niakousari:** Supervision.

Declaration of competing interest

The authors declare no conflicts of interest.

Acknowledgements

This research project was financially supported by Shiraz University.

Appendix A. Supplementary data

Supplementary data to this article can be found online at https://doi.org/10.1016/j.fochx.2025.102495.

Data availability

Data will be made available on request.

References

Abdullah, M. S. P., Noordin, M. I., Ismail, S. I. M., Mustapha, N. M., Jasamai, M., Danik, M. F., … Shamsuddin, A. F. (2018). Recent advances in the use of animal-sourced gelatine as natural polymers for food, cosmetics and pharmaceutical applications. *Sains Malaysiana, 47*(2), 323–336.

Ahmad, T., Ismail, A., Ahmad, S. A., Khalil, K. A., Kee, L. T., Awad, E. A., & Sazili, A. Q. (2020). Extraction, characterization and molecular structure of bovine skin gelatin extracted with plant enzymes bromelain and zingibain. *Journal of Food Science and Technology, 57*, 3772–3781.

Akman, P. K., Bozkurt, F., Balubaid, M., & Yilmaz, M. T. (2019). Fabrication of curcumin-loaded gliadin electrospun nanofibrous structures and bioactive properties. *Fibers and Polymers, 20*, 1187–1199.

Amani, F., Rezaei, A., Akbari, H., Dima, C., & Jafari, S. M. (2022). Active packaging films made by complex Coacervation of Tragacanth gum and gelatin loaded with curcumin; characterization and antioxidant activity. *Foods, 11*(20), 3168.

Ashayerizadeh, O., Dastar, B., & Pourashouri, P. (2020). Study of antioxidant and antibacterial activities of depolymerized fucoidans extracted from Sargassum tenerrimum. *International Journal of Biological Macromolecules, 151*, 1259–1266.

Golmakani, M.-T., Hajjari, M. M., Kiani, F., Sharif, N., & Hosseini, S. M. H. (2024). Application of electrospinning to fabricate phycocyanin- and Spirulina extract-loaded gliadin fibers for active food packaging. *Food Chemistry: X, 22*, Article 101275.

Golmakani, M.-T., Kiani, F., Hajjari, M. M., Sharif, N., Fazaeli, M., & Hosseini, S. M. H. (2023). Electrospun zein incorporating phycocyanin and Spirulina extract: Fabrication, characterization, and potential application. *LWT, 188*, Article 115408.

Hajjari, M. M., Golmakani, M.-T., & Sharif, N. (2021). Fabrication and characterization of cuminaldehyde-loaded electrospun gliadin fiber mats. *LWT, 145*, Article 111373.

Hajjari, M. M., Golmakani, M.-T., & Sharif, N. (2023). Electrospun zein/C-phycocyanin composite: Simulation, characterization and therapeutic application. *Food Hydrocolloids, 140*, Article 108638.

Hajjari, M. M., Golmakani, M.-T., Sharif, N., & Niakousari, M. (2021). In-vitro and in-silico characterization of zein fiber incorporating cuminaldehyde. *Food and Bioproducts Processing, 128*, 166–176.

Hajjari, M. M., & Sharif, N. (2021). In-silico behavior of dissolved prolamins under electric field effect applied by electrospinning process using molecular dynamics simulation. *Journal of Molecular Liquids, 344*, Article 117778.

Hajjari, M. M., & Sharif, N. (2022). In-silico zein/tannic acid colloidal nanoparticles and their activity at oil and water interface of Pickering emulsion using molecular dynamics simulation. *Journal of Molecular Liquids, 359*, Article 119321.

Hajjari, M. M., & Sharif, N. (2024). Prolamins' 3D structure: A new insight into protein modeling using the language of numbers and shapes. *Food Hydrocolloids, 154*, Article 110154.

Hifney, A. F., Fawzy, M. A., Abdel-Gawad, K. M., & Gomaa, M. (2016). Industrial optimization of fucoidan extraction from Sargassum sp. and its potential antioxidant and emulsifying activities. *Food Hydrocolloids, 54*, 77–88.

Ho, T. C., Lim, J.-S., Kim, S.-J., Kim, S.-Y., & Chun, B.-S. (2023). In Vitro Biodegradation, Drug Absorption, and Physical Properties of Gelatin–Fucoidan Microspheres Made of Subcritical-Water-Modified Fish Gelatin. *Marine Drugs, 21*(5), 287.

Kazemian-Bazkiaee, F., Ebrahimi, A., Hosseini, S. M., Shojaee-Aliabadi, S., Farhoodi, M., Rahmatzadeh, B., & Sheikhi, Z. (2020). Evaluating the protective effect of edible coatings on lipid oxidation, fatty acid composition, aflatoxins levels of roasted peanut kernels. *Journal of Food Measurement and Characterization, 14*, 1025–1038.

Kramer, R. Z., Bella, J., Mayville, P., Brodsky, B., & Berman, H. M. (1999). Sequence dependent conformational variations of collagen triple-helical structure. *Nature Structural Biology, 6*(5), 454–457.

Liu, K., Liu, Y., & Chen, F. (2019). Effect of storage temperature on lipid oxidation and changes in nutrient contents in peanuts. *Food Science & Nutrition, 7*(7), 2280–2290.

Liu, M., Liu, Y., Cao, M.-J., Liu, G.-M., Chen, Q., Sun, L., & Chen, H. (2017). Antibacterial activity and mechanisms of depolymerized fucoidans isolated from Laminaria japonica. *Carbohydrate Polymers, 172*, 294–305.

Luo, Q., Hossen, M. A., Zeng, Y., Dai, J., Li, S., Qin, W., & Liu, Y. (2022). Gelatin-based composite films and their application in food packaging: A review. *Journal of Food Engineering, 313*, Article 110762.

Malde, A. K., Zuo, L., Breeze, M., Stroet, M., Poger, D., Nair, P. C., … Mark, A. E. (2011). An automated force field topology builder (ATB) and repository: Version 1.0. *Journal of Chemical Theory and Computation, 7*(12), 4026–4037.

Mani, G., Rajendran, I., Jayakumar, T., Mani, A., Govindaraju, R., & Dhayalan, S. (2024). Evaluation of antibiofilm and antiquorum sensing activities of fucoidan characterized from Padina boryana against nosocomial pathogens. *Applied Biochemistry and Biotechnology, 196*(8), 4727–4744.

Masek, A., Chrzescijanska, E., & Zaborski, M. (2013). Characteristics of curcumin using cyclic voltammetry, UV–vis, fluorescence and thermogravimetric analysis. *Electrochimica Acta, 107*, 441–447.

Perera, K. Y., Sharma, S., Pradhan, D., Jaiswal, A. K., & Jaiswal, S. (2021). Seaweed polysaccharide in food contact materials (active packaging, intelligent packaging, edible films, and coatings). *Foods, 10*(9), 2088.

Pouralkhas, M., Kordjazi, M., Ojagh, S. M., & Farsani, O. A. (2023). Physicochemical and functional characterization of gelatin edible film incorporated with fucoidan isolated from Sargassum tenerrimum. *Food Science & Nutrition, 11*(7), 4124–4135.

Ravikumar, K., Humphrey, J., & Hwang, W. (2007). Spontaneous unwinding of a labile domain in a collagen triple helix. *Journal of Mechanics of Materials and Structures, 2*(6), 999–1010.

Roy, S., & Rhim, J.-W. (2020). Preparation of antimicrobial and antioxidant gelatin/curcumin composite films for active food packaging application. *Colloids and Surfaces B: Biointerfaces, 188*, Article 110761.

Sabaghi, M., Maghsoudlou, Y., Khomeiri, M., & Ziaiifar, A. M. (2015). Active edible coating from chitosan incorporating green tea extract as an antioxidant and antifungal on fresh walnut kernel. *Postharvest Biology and Technology, 110*, 224–228.

Sangatash, M. M., Niazmand, R., Jamab, M. S., & Modaressi, A. S. (2016). Development of antioxidant active films containing sodium ascorbate (SA) and ethylene vinyl alcohol (EVOH) to extend the shelf life of peanut. *Journal of Food Science and Technology, 53*(4), 1766–1783.

Sharif, N., Golmakani, M. T., & Hajjari, M. M. (2022). Integration of physicochemical, molecular dynamics, and in vitro evaluation of electrosprayed γ-oryzanol-loaded gliadin nanoparticles. *Food Chemistry, 395*, Article 133589.

Sharif, N., Golmakani, M.-T., Hajjari, M. M., Aghaee, E., & Ghasemi, J. B. (2021). Antibacterial cuminaldehyde/hydroxypropyl-β-cyclodextrin inclusion complex electrospun fibers mat: Fabrication and characterization. *Food Packaging and Shelf Life, 29*, Article 100738.

Siripatrawan, U., & Harte, B. R. (2010). Physical properties and antioxidant activity of an active film from chitosan incorporated with green tea extract. *Food Hydrocolloids, 24*(8), 770–775.

Wang, F., Xie, C., Tang, H., Li, H., Hou, J., Zhang, R., Liu, Y., & Jiang, L. (2023). Intelligent packaging based on chitosan/fucoidan incorporated with coleus grass (Plectranthus scutellarioides) leaves anthocyanins and its application in monitoring the spoilage of salmon (Salmo salar L.). *International Journal of Biological Macromolecules, 252*, Article 126423.

Woods, R. (2005). *Glycam web. Complex carbohydrate research center*. Athens, GA: University of Georgia.

Zhang, X., Li, Y., Guo, M., Jin, T. Z., Arabi, S. A., He, Q., … Liu, D. (2021). Antimicrobial and UV blocking properties of composite chitosan films with curcumin grafted cellulose nanofiber. *Food Hydrocolloids, 112*, Article 106337.

Zhao, M., Garcia-Vaquero, M., Przyborska, J., Sivagnanam, S. P., & Tiwari, B. (2021). The development of analytical methods for the purity determination of fucoidan extracted from brown seaweed species. *International Journal of Biological Macromolecules, 173*, 90–98.

Zheng, Y., Yao, F., & Chen, F. (2022). Curcumin-loaded electrospun peanut protein isolate/poly-l-lactic acid nanofibre membranes: Preparation and characterisation and release behaviour. *LWT, 169*, Article 113978.

Zhou, Y., Miao, X., Lan, X., Luo, J., Luo, T., Zhong, Z., Wang, H., & Tang, Y. (2020). Angelica essential oil loaded electrospun gelatin nanofibers for active food packaging application. *Polymers, 12*(2), 299.